

Scaling up Privacy-Preserving ML: A CKKS Implementation of Llama-2-7B

Jaiyoung Park

Graduate School of Convergence
Science and Technology, Seoul
National University
Seoul, South Korea

Jung Ho Ahn

Graduate School of Convergence
Science and Technology, Seoul
National University
Seoul, South Korea

Jung Woo Kim

CryptoLab, Inc.
Seoul, South Korea

Sejin Park

CryptoLab, Inc. & Seoul National
University
Seoul, South Korea

Jung Hee Cheon

Cryptolab, Inc. & Departement of
Mathematics, Seoul National
University
Seoul, South Korea

Minje Park

CryptoLab, Inc.
Seoul, South Korea

Jai Hyun Park

CryptoLab, Inc.
Lyon, France

Guillaume Hanrot

CryptoLab, Inc.
Lyon, France

Damien Stehlé

CryptoLab, Inc.
Lyon, France

Abstract

As large language models (LLMs) become ubiquitous, privacy concerns pertaining to inference inputs keep growing. In this context, fully homomorphic encryption (FHE) has emerged as a primary cryptographic solution to provide non-interactive confidential LLM inference. Existing solutions scale poorly with the input token length, and hence focus either on small models or larger models with a small number of input tokens. They also suffer from the existence of large outlier values. These values have a strong impact on the evaluation of non-linear layers, leading to large-degree polynomial approximation and thus heavy evaluation costs.

We propose an FHE-based private LLM inference solution that allows thousands of input tokens with only a part of them being encrypted: this fits with a scenario where the context is benign and only part of the input is sensitive. To do so, we suggest an unbalanced chunked prefill framework that processes the private and public parts of the input tokens differently. Our framework contains plaintext-plaintext, plaintext-ciphertext and ciphertext-ciphertext computational components. We adopt different strategies and ingredients for each component. We also devise new homomorphic algorithms for specific matrix multiplication and polynomial evaluation tasks encountered during LLM inference.

Furthermore, without retraining, we tailor the LLM inference algorithm to reduce the ranges of outlier values: we leverage machine learning strategies (token prepending and rotations) to mitigate the impact of the outliers on non-linear layers.

Based on these ingredients, we describe a CKKS-based end-to-end implementation of Llama-2-7B private inference for up to 4096 input tokens, of which the last 128 are encrypted. On a cluster of 8 NVIDIA RTX-4090 GPUs, inference takes 85s for summarization and 33s for generation per output token. As a comparison, on the similar-size Llama-3-8B, Jayashankar *et al* [arxiv'25] perform summarization for only 128 tokens in 295s on 8 (much costlier) H100 GPUs. For the smaller BERT-base model, Moon *et al* [CCS'25] handle 128 input tokens in 602s on an A100 GPU.

1 Introduction

When querying a Large Language Models (LLM), clients typically send queries to a computing server that runs the model inference. As these queries and their results often contain sensitive data, privacy concerns emerge. For this reason, various attempts have been made in the last few years at obtaining privacy-preserving LLM inference. These often rely on MPC (secure multi-party computation) and some FHE (fully homomorphic encryption) components, or on FHE only. MPC solutions [HLL⁺23, WFZ⁺, KC25, CXS⁺25, DjLZ⁺25, GJM⁺24, ZYH⁺25, LHG⁺25, XLL⁺25, YZL23] suffer from two major drawbacks: they involve many rounds of communication with the client during the computation, and they assume that the computing parties do not collude. Oppositely, the FHE computation is public and incurs minimal interaction. In this work, we focus on inference using the CKKS FHE scheme [CKKS17].

Prior works show limited performance, even though they focus on small LLMs. Several studies [CBH⁺22, MYJK25, PLL25, YCD⁺25, ZWS⁺25] consider BERT, and only a few address (significantly larger) small Llama models [TLI⁺23]. When they do so, it is typically with only a few input tokens (e.g., 8 in [ZYH⁺25, ZWS⁺25]). Even for these small LLMs, obtaining a practical implementation remains a challenge due to the massive size of the computation. For example, the NEXUS protocol from [ZYH⁺25] requires 51.84s of amortized time per token for the Llama-3-8B model, using four A100 GPUs, with 8 input tokens. The MOAI protocol from [ZWS⁺25] requires 224.53s for processing 8 input tokens on the Llama-3-8B model on a single A100 GPU. A recent work [JKS⁺25] implemented FHE-based private inference of Llama-3-8B with 128 input tokens, taking 295s using 8 H100 GPUs or 134s using 8 B200 GPUs.

Given these runtimes, increasing the number of input tokens seems challenging: some components have a cost that grows linearly in the number of input tokens, while others (at the core of the attention phase) have costs that grow quadratically. Furthermore, increasing the model size and the number of tokens leads to robustness difficulties. Larger models lead to larger ranges of

values for intermediate variables [SCKL24], because of outliers that largely exceed the average magnitudes. These directly impact the efficiency of FHE inference, through increased degrees of polynomial approximations, increased ciphertext modulus consumption, and ciphertext maintenance costs.

1.1 Contributions

We leverage machine learning techniques and develop specific FHE algorithms to enable the inference of Llama models with a large number of input tokens. To enable more input tokens while limiting the efficiency impact, we provide some of them as plaintexts and others as ciphertexts. Our implementation, running on a cluster of 8 RTX-4090 GPUs connected through PCI links, is capable of processing 4096 input tokens of which only the last 128 are encrypted, in 85s for prefill summarization and 33s for generation.

The hybrid plaintext/ciphertext status of input tokens reflects a situation where the client formulates complex requests in a generic public form and postpones the specific confidential elements to the end of the prompt, where they are processed in encrypted form. Compared to evaluating an LLM with only some moderate number of encrypted input tokens, this modification mostly impacts the attention phase of the LLM evaluation. During this phase, each value manipulated is derived from a pair of input tokens. When at least one of them is encrypted, so is the manipulated value; as a consequence, the amount of encrypted information grows as a function of the total input size (not only as a function of the number of encrypted tokens). From an FHE evaluation perspective, the width of the circuit at this stage is very large, leading to aggressive optimization strategies. As bootstrapping [CHK¹⁸] is the most expensive component of CKKS, we design an (almost) bootstrap-free attention phase for Llama models; only the Softmax evaluation, in its batched version [CHK²⁴], retains a small number of bootstraps. To do so, we devise an optimized plaintext-ciphertext matrix multiplication algorithm with affordable memory footprints for LLM inference. An additional contribution is to compute Softmax using a new polynomial evaluation algorithm designed for ciphertexts with few slots, consuming only $O(\log d)$ homomorphic operations, where d is the degree of the polynomial to be evaluated.

Additionally to these algorithmic modifications, we also use machine-learning techniques to reduce the input range of nonlinear functions. Namely, we apply rotations of the ambient space in the LLM evaluation flow and we prepend “faulty tokens” to the input. These techniques allow us to decrease the ranges of intermediate variables. Further, extensive experiments allowed us to carefully select plaintext precisions that are as low as possible while preserving inference quality. The CKKS scaling factors and bootstrap parameters have been optimized on the basis of these ranges and precisions.

1.2 Technical overview

FHE-based LLM inference generates encrypted output tokens from the given encrypted input tokens. Scaling it up creates two main difficulties: the increased magnitudes of outliers in the scaled models must be taken care of to provide robust FHE inference, and the ciphertext-ciphertext computations can incur a computational blow-up.

Tailoring LLM models. The cost of FHE computations increases when handling outliers from scaled LLMs. FHE bootstrapping must support higher relative precision: even though some dedicated algorithms exist [BCC²², CKSS²⁵], their cost is significantly higher than regular CKKS bootstrapping. Further, as CKKS supports only addition and multiplication, computing non-arithmetic functions is performed via polynomial approximation; another cost increase stems from polynomial approximations on larger intervals [CKP²²]: the existence of outliers implies that the domain for approximation should be wide, resulting in higher-degree approximation polynomials.

To this end, we tailor LLM models to tame the outliers and moderate their impact. For this purpose, we adopt machine learning techniques. First, following [XTC²⁴], we prepend “faulty tokens” to the inputs, yielding a better initial Key-Value cache that mitigates outlier values during computation. Second, following [AMC²⁴], we adaptively rotate the ambient space of LLM to spread the potential impact of the outlier coordinate to many other coordinates. Using these two techniques, we keep the size of all intermediate encrypted values reasonably small, avoiding a high increase of the cost of homomorphic algorithms for outliers.

Heterogeneous chunked prefill stages. The remaining issue is the significant computational overhead associated with ciphertext-ciphertext computations. Compared to plaintext-ciphertext computations, both the operations and the algorithms for ciphertext-ciphertext computations are much more expensive; for example, ciphertext-ciphertext matrix multiplication [JKLS18, Par25] is heavier than plaintext-ciphertext matrix multiplications [BCH²⁴].

To this end, we propose heterogeneous chunked prefill stages. The main goal is to encrypt only part of the input tokens. This fits with applications where the context is benign and only a part of the input is sensitive. Then, we split the prefill stage of LLM into two: the public prefill stage and the private prefill stage. The unencrypted input tokens are handled by the public prefill stage in the clear, generating the clear Key-Value cache. From the Key-Value cache and the remaining encrypted input tokens, the private prefill stage generates the encrypted output tokens. Our heterogeneous chunked prefill stages were inspired by the chunked prefill technique from [APM²³], which splits the prefill stage into several chunks for a better pipeline parallel schedule. In contrast to [APM²³], our chunks are highly unbalanced: we aim at a large public prefill stage with many benign input tokens and a small private prefill stage with a few encrypted input tokens.

The prefill stages consist of four steps: QKV generation, attention operation, O-projection, and feed-forward network (FFN). In the private prefill stage, the most costly step is the attention operation, which comprises plaintext-ciphertext component (PC-attention) and ciphertext-ciphertext component (CC-attention). In components other than PC-attention, we focus on collecting and making full use of a number of recent FHE techniques [BCH²⁴, CHK²⁴, HYT²⁴, CCK²⁵] in order to offer state-of-the-art performance. Also, we perform computationally expensive components with the smallest CKKS parameters possible and place bootstraps in strategic places.

Almost bootstrap-free PC-attention. Each FHE ciphertext is associated to a certain ciphertext modulus, which decreases at each

homomorphic multiplication. Once it runs out of modulus, the ciphertext needs to be bootstrapped. This bootstrapping procedure is more expensive than other homomorphic operations, in particular compared to plaintext-ciphertext operations.

PC-attention mostly contains plaintext-ciphertext operations. The increased number of plaintext input tokens results in a large plaintext Key-Value cache. As a result, the PC-attention circuit is wide. If we need to bootstrap the ciphertexts during PC-attention, then many ciphertexts will be involved, leading to a large number of bootstraps. We aim for PC-attention with as few bootstraps as possible, by making it shallow in terms of homomorphic multiplications. To achieve (almost) bootstrapping-free PC-attention, we devise a new plaintext-ciphertext matrix multiplication (PCMM) algorithm adapted from [JKLS18] and a Softmax evaluation algorithm adapted from [CHK⁺24]. Overall, we perform a very small number of bootstraps in the auxiliary track of the algorithm from [CHK⁺24].

Shallow PCMM with affordable memory footprint. The state-of-the-art PCMM algorithms from [BCH⁺24] are shallow, but they require modulus-consuming data encoding conversions for the subsequent Softmax evaluation when avoiding bootstraps. The PCMM algorithms in [MYJK25] and [JKLS18] do not require encoding conversion, but they consume 2 or 3 multiplicative levels. The PCMM algorithm in [PLL25] is shallow, does not require encoding conversion, and is computationally cheaper than [MYJK25, JKLS18]. However, including [PLL25], all the above algorithms except [BCH⁺24] suffer from a massive memory footprint: they rely on duplicated plaintext matrices. Since we avoid any bootstraps, we need to perform some PCMMs with a rather large ciphertext modulus, and such large memory requirements are unaffordable.

We devise a new PCMM algorithm specifically for PC-attention. It consumes a single multiplicative level without any encoding conversion. To obtain this minimalistic multiplicative depth, in contrast to [JKLS18], we allow our PCMM algorithm to flexibly update the packing structure of underlying FHE ciphertexts. Moreover, we adopt baby-step giant-step hoisting to achieve the same asymptotic complexity as [PLL25], which is less than that of [JKLS18, MYJK25]. Precisely, to multiply an encrypted matrix M by a cleartext matrix U of dimension $d \times d$, we observe that the product matrix $U \cdot M$ is identical to

$$\tau \left(\sum_{j=0}^{g-1} \text{Rot}_{\text{row}}^{j \cdot b} \left(\sum_{i=0}^{b-1} \left(\text{Rot}_{\text{row}}^{-\ell \cdot (i+j \cdot b) - j \cdot b} \circ \text{Rot}_{\text{col}}^{i+j \cdot b} (U') \right) \circ \text{Rot}_{\text{row}}^i (M) \right) \right) ,$$

where τ is a fixed linear transformation and U' is a matrix depending on U . Note that b and g are constants satisfying $b \cdot g = d$, Rot_{row} and Rot_{col} are rotations of rows and columns of a matrix, and \circ refers to coefficient-wise multiplication of matrices stored as vectors by writing rows after rows. We are storing only U' rather than copies of U with rotations, which makes the memory footprint of PCMMs reasonable even at large moduli.¹

Shallow Softmax and slim polynomial evaluation. We optimize the homomorphic Softmax algorithm from [CHK⁺24] by

¹It is possible to apply our on-the-fly PCMM technique to [PLL25] to solve the memory-related issue. However, the resulting PCMM algorithm requires more plaintext rotations than ours. Note that, although it is cheaper than for ciphertexts, each plaintext rotation involves a complicated memory access pattern, whose cost is not negligible in GPU implementations.

exploiting the sharp control of the ranges of inputs and intermediate values in the calls to Softmax in the Llama models. Recall that the algorithm from [CHK⁺24] consists of two tracks: a wide main track and a slim-but-deep auxiliary track. The control on the ranges of variables leads to a shallow main track.

We optimize the auxiliary track by leveraging the fact that the corresponding ciphertexts are sparsely packed, i.e., their message dimension is much smaller than the ciphertext capacity. For this purpose, we introduce a slim polynomial evaluation algorithm for sparsely packed ciphertexts. The main idea is to use the superfluous message slots for the purpose of the computation. This is achieved by (recursively) decomposing the polynomial to be evaluated as a sum of squares of two other polynomials of half degree, and evaluating these two polynomials in parallel.

2 Preliminaries

We use boldface letters for vectors and capital letters for matrices. The vector spaces \mathbb{R}^n and \mathbb{C}^n are equipped as rings with coordinate-wise addition and multiplication (denoted by \odot). We let $\lfloor \cdot \rfloor$ denote rounding to nearest (with an arbitrary rule for ties). The base-2 logarithm is denoted by \log . Throughout the paper, we abbreviate the multiplication between a plaintext matrix and a ciphertext matrix as PCMM, that between ciphertext matrices as CCMM, that between a plaintext vector and a ciphertext matrix as PCMv, and that between ciphertext vector and matrix as CCMv.

2.1 The CKKS scheme

CKKS [CKKS17] is an RLWE-based fully homomorphic encryption scheme implementing arithmetic over approximate (real or complex) numbers. Its main parameter is the ring degree $N = 2^n$ (typically $n = 16$). It has message space $\mathbb{C}^{N/2}$, while its plaintext space is $\mathcal{R}_N = \mathbb{Z}[X]/(X^N + 1)$ – we shall simply use \mathcal{R} when there is no ambiguity on the ring degree.

2.1.1 Encodings. Let $\zeta = \exp(i\pi/N)$ be a primitive $(2N)$ -th root of unity. We define the map $\text{iDFT} : \mathbb{C}^{N/2} \rightarrow \mathbb{R}[X]/(X^N + 1)$ by

$$P = \text{iDFT}((\mathbf{m})_{0 \leq i < N/2}) \Leftrightarrow P(\zeta^{5^i}) = m_i, \quad 0 \leq i < N/2 .$$

CKKS maps the message space to the plaintext space using one of the following two encoding functions, parameterized by a large integer Δ called the *scaling factor* and which drives the numerical precision. On input $\mathbf{m} = (m_i)_{0 \leq i < N/2}$, we define

$$\text{Ecd}_{\text{slot}}(\mathbf{m}) = \lfloor \Delta \cdot \text{iDFT}(\mathbf{m}) \rfloor ,$$

$$\text{Ecd}_{\text{coeff}}(\mathbf{m}) = \sum_{i=0}^{N/2-1} (\lfloor \Delta \cdot \text{Re}(\mathbf{m}_i) \rfloor + X^{N/2} \lfloor \Delta \cdot \text{Im}(\mathbf{m}_i) \rfloor) \cdot X^i .$$

Both slot and coeff encodings map messages to plaintexts.

The approximate inverse of this map (up to rounding) will be denoted by Dcd_{slot} and $\text{Dcd}_{\text{coeff}}$, respectively. The approximate relations

$$\begin{aligned} \text{Ecd}_{\text{slot}}(\mathbf{m}_1 + \mathbf{m}_2) &\approx \text{Ecd}_{\text{slot}}(\mathbf{m}_1) + \text{Ecd}_{\text{slot}}(\mathbf{m}_2) , \\ \text{Ecd}_{\text{slot}}(\mathbf{m}_1 \odot \mathbf{m}_2) &\approx \Delta \cdot (\text{Ecd}_{\text{slot}}(\mathbf{m}_1) \cdot \text{Ecd}_{\text{slot}}(\mathbf{m}_2)) \end{aligned} \quad (1)$$

illustrate that, up to an extra term Δ for multiplication, the function Ecd_{slot} is an approximate ring homomorphism from the message

space to the plaintext space, where the multiplication \odot in the message space is componentwise multiplication. In the sequel, when we use Ecd , Dcd without further indication, we refer to slot encoding.

When the message to be encoded has fewer coordinates than $N/2$, we call it slim. This terminology is extended to plaintexts (and ciphertexts) if their underlying messages are slim. Algebraically, if N' is the smallest power of two that is no smaller than the number of coordinates, we have the plaintext live in a subring $\mathcal{R}_{N'}$ of \mathcal{R}_N ; equivalently, when using slot-encoding the underlying message is periodic, of the form

$$(x_0, \dots, \underbrace{x_{N'/2-1}, x_0, \dots, x_{N'/2-1}}_{N/N' \text{ times}}, \dots, x_0, \dots, x_{N'/2-1}) \dots$$

In this work, as we have no use for complex numbers, we shall use the conjugate-invariant version of CKKS [KS18]; the latter can be seen as a variant on top of ordinary CKKS, giving access to N real slots rather than $N/2$ complex slots while keeping the fact that slot encoding is an approximate ring homomorphism. This induces a number of technicalities for which the interested reader is referred to [KS18].

2.1.2 Encryption and decryption. CKKS uses RLWE ciphertext formats [STX09, LPR10]²

- **SetUp:** chooses a tuple $(N, P, Q, h, \mathcal{D})$, where N, P, Q , and h are positive integers (respectively ring degree, auxiliary modulus, top ciphertext modulus, and secret key Hamming weight) and \mathcal{D} is a distribution on \mathcal{R} . These parameters are chosen so that RLWE with ring degree N and modulus PQ with sparse ternary secrets of Hamming weight h and error distribution \mathcal{D} has 128-bit security. Setup also picks and returns a uniform $\text{sk} \in \mathbb{Z}[X]/(X^N + 1)$ with coefficients in $\{-1, 0, 1\}$ and h non-zero coefficients. The choice of (N, P, Q) among secure values takes into account the circuit to be implemented, in particular its shape in terms of width (related to N), depth (related to Q), and number of key switchings (the cost of which is related to an integer parameter $\text{dnum} \approx (\log Q)/(\log P)$).
- **Enc_{sk, D, Q}(pt):** on input $\text{pt} \in \mathbb{Z}[X]/(X^N + 1)$, return a pair $(a, -a \cdot \text{sk} + \text{pt} + e \bmod Q)$, where $e \leftarrow \mathcal{D}$ and a is uniformly chosen in $\mathcal{R}_Q = \mathcal{R}/Q\mathcal{R}$;
- **Dec_{sk}(ct):** on input $\text{ct} = (a, b) \in \mathcal{R}_Q^2$, return $a \cdot \text{sk} + b \bmod Q$.

In particular, the CKKS ciphertext space is \mathcal{R}_Q^2 . For simplicity, we omit the possibility to enable public key encryption, and encryption/decryption with various moduli. In the sequel, we shall simply write Enc and Dec , and assume that all their parameters are fixed at setup time.

An important property of RLWE ciphertexts for homomorphic encryption is the ability to switch keys. A *key-switching key* from the secret key sk to the secret key sk' is an encryption of $P \cdot \text{sk}'$ under sk in \mathcal{R}_{PQ}^2 , namely a pair $(a, -a \cdot \text{sk} + P \cdot \text{sk}' + e)$, where $e \leftarrow \mathcal{D}$ and a is uniformly chosen in \mathcal{R}_{PQ} (assuming that $\text{dnum} = 1$). This key-switching key, which can be made public, is used in the key-switching operation:

²Some functionalities require moving to MLWE formats [BGV14, LS15] temporarily.

- **KeySwitch_{ksk}(ct):** on input a key-switching key ksk from sk' in \mathcal{R}_{PQ}^2 and a ciphertext $\text{ct} \in \mathcal{R}_Q^2$ encrypted under sk , returns a ciphertext $\text{ct}' \in \mathcal{R}_Q^2$ under sk' such that $\text{Dec}_{\text{sk}'}(\text{ct}') \approx \text{Dec}_{\text{sk}}(\text{ct})$. KeySwitch reduces to arithmetic in \mathcal{R}_{PQ} , with a number of operations depending on dnum .

2.1.3 Homomorphic functionalities. CKKS offers the following homomorphic functionalities.

- **Add(ct₁, ct₂):** on input two ciphertexts ct_1 and ct_2 in \mathcal{R}_Q^2 , return a ciphertext $\text{ct} \in \mathcal{R}_Q^2$ such that $\text{Dec}(\text{ct}_{\text{res}}) \approx \text{Dec}(\text{ct}_1) + \text{Dec}(\text{ct}_2)$; this operation is implemented as componentwise addition in \mathcal{R}_Q^2 ;
- **PCMult(pt, ct):** on input a plaintext $\text{pt} \in \mathcal{R}$ and a ciphertext $\text{ct} \in \mathcal{R}_Q$, both with scaling factor Δ , return a ciphertext $\text{ct}' \in \mathcal{R}_{Q'}^2$ with $Q' \approx Q/\Delta$, such that $\text{Dcd}(\text{Dec}(\text{ct}')) \approx \text{Dcd}(\text{Dec}(\text{ct})) \odot \text{Dcd}(\text{pt})$.
- **Mult_{rlk}(ct₁, ct₂):** on input two ciphertexts ct_1 and ct_2 in \mathcal{R}_Q^2 with scaling factors Δ , and a key-switching key $\text{rlk} \in \mathcal{R}_{PQ}^2$ from sk^2 to sk , return a ciphertext $\text{ct}' \in \mathcal{R}_{Q'}^2$ with $Q' \approx Q/\Delta$, such that $\text{Dcd}(\text{Dec}(\text{ct}')) \approx \text{Dcd}(\text{Dec}(\text{ct}_1)) \odot \text{Dcd}(\text{Dec}(\text{ct}_2))$.
- **Rot_{rlk}(ct, k):** on input a ciphertext ct , an integer $0 \leq k < N/2$, and a switching key from $\text{sk}(X^{5^k})$ to sk , return a ciphertext ct' such that $\text{Dcd}(\text{Dec}(\text{ct}'))$ is a cyclic rotation of $\text{Dcd}(\text{Dec}(\text{ct}))$ by k positions.

2.1.4 Rescaling, precision, and modulus handling. The use of a scaled encoding with scaling factor Δ implies that the arithmetic result of an encoded multiplication must be corrected via division by Δ in order to restore the correct encoding (see Equation (1)). This is implemented homomorphically as Rescale:

- **Rescale(ct):** on input a ciphertext $\text{ct} \in \mathcal{R}_Q^2$, returns $\text{ct}' \in \mathcal{R}_{Q'}^2$ with $Q' \approx Q/\Delta$, such that $\text{Dec}(\text{Dcd}(\text{ct}')) \approx \Delta^{-1} \cdot \text{Dec}(\text{Dcd}(\text{ct}))$.

As a consequence, every multiplication reduces the modulus of a ciphertext by a factor $\approx \Delta$. This is usually accounted via the notion of *level*: given integers Q_0, Q_1, \dots, Q_L where $Q_i/Q_{i-1} \approx \Delta$ for $i \geq 1$, we define level- j ciphertexts as elements of $\mathcal{R}_{Q_j}^2$. Multiplication (both PCMult and Mult) can then be seen as taking its inputs in $\mathcal{R}_{Q_j}^2$ and returning its result in $\mathcal{R}_{Q_{j-1}}^2$.

The numerical model of CKKS is close to a fixed-point number system, meaning that the precision of an input value x is absolute and does not depend on the order of magnitude of x . The precision of CKKS computations is driven by the scaling factor Δ . Choosing Δ is a tradeoff between precision needs and modulus usage: a larger Δ provides better accuracy but exhausts ciphertext modulus faster.

2.1.5 Bootstrapping. The maximal modulus PQ that can be used for a fixed N is bounded from above for security reasons; combined with the discussion in Section 2.1.4, this implies that a ciphertext eventually reaches level 0, namely modulus Q_0 , after sufficiently many multiplications; at this stage, this ciphertext can no longer be multiplied unless it undergoes modulus restoration, called bootstrapping. CKKS bootstrapping [CHK⁺18] is a complex and costly operation, which often accounts for a large proportion of the total

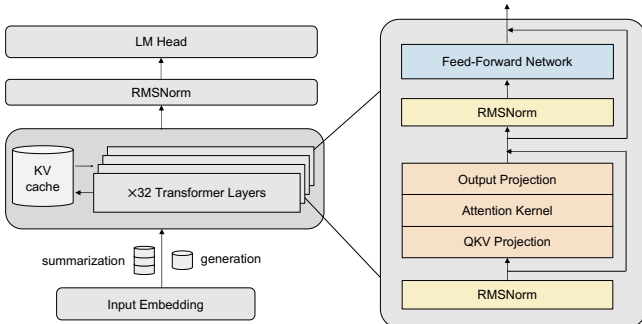


Figure 1: Llama model architecture

cost of deep homomorphic circuits. As such, organizing the computation so as to minimize the number of bootstraps is often a key to the design of efficient homomorphic algorithms.

The bootstrapping process uses a significant part of the modulus that it restores, with a total amount usage directly connected to its precision. CKKS bootstrapping, when called on a ciphertext ct , assumes that its input has all its slots in $[-1, 1]$; if this condition is not fulfilled, the precision of the corresponding slot value degrades quickly. One can handle larger values with large-precision bootstrapping [BCC⁺22, CKSS25], but this increases the cost significantly.

2.2 Llama-2-7B and Llama-3-8B

We focus on Llama-2 and Llama-3 for evaluating LLM inference throughout the paper. Llama models follow a decoder-only transformer architecture [VSP¹⁷] with 32 layers, a model dimension of 4096, 32 attention heads, and a hidden dimension of 11008 (Llama-2-7B) or 14336 (Llama-3-8B) in the feed-forward network. It adopts pre-normalization using root mean square normalization (RMSNorm), rotary positional embeddings (RoPE), and SwiGLU activation (a SiLU-gated linear unit) in the feed-forward network (FFN). Llama models share core architectural components with more recent LLMs, which makes it a lightweight yet representative model, suitable for our analysis of inference dynamics and FHE execution.

Llama follows the standard autoregressive inference, generating one token per forward pass. The first forward pass is specifically referred to as prefill stage, which processes the entire input sequence and produces the first output token. The subsequent passes are called decode stage. By the causal attention mechanism, token computation involves only preceding tokens, specifically Key (K) and Value (V) vectors. Without optimization, the N -th forward pass consists of the same computation as the $(N - 1)$ -th pass plus the computation of the N -th token. The standard KV-caching optimization caches the intermediate Key-Value result of the $(N - 1)$ -th pass and performs the computation for the N -th token only, mitigating redundant computation for each step.

3 Tailoring Llama for Encrypted Inference

In this section, we detail our approach to stabilize activation function outliers. First, we conduct an empirical characterization of Llama models to define numerical targets for FHE circuits, such

Table 1: Maximal input magnitudes of non-linear layers with and without prefix optimization.

Position	Baseline	With Prefixing	Reduction
SoftMax	39.24	32.78	-16%
SiLU	23.00	10.82	-53%
RMSNorm	2243.97	7.65	-99.7%

as dynamic range and bit-precision, required to preserve model accuracy. This insight allows us to set specific parameters for fitting robust polynomial approximations and precision-aware bootstrapping, ensuring consistent verification of the whole pipeline.

3.1 Outlier mitigation

LLMs are known to exhibit substantially large activation input values during inference, a behavior referred to as the *outlier phenomenon* [SCKL24]. These drastic dynamics, intrinsic to the LLM architecture, create a significant challenge for generating both efficient and accurate FHE circuits: the outliers lead to high-degree polynomial approximations, which are costly to evaluate for all inputs. We address this by repurposing activation smoothing techniques [XTC²⁴, AMC²⁴, XLS²³] from the LLM optimization domain, tailoring them to meet the FHE stability requirements.

The first category of outliers stems from the *attention sink* phenomenon [XTC²⁴]. These outliers are characterized by scalars with extreme magnitudes, which could be larger than 1,000 in Llama-2-7B [TMS²³], and are triggered when special tokens are processed for the first time during inference. We mitigate this by prepending a specialized prefix—injecting a short, precomputed Key-Value cache derived from the specific tokens that induce this sink behavior. This approach ensures that the model operates in a stabilized regime, effectively smoothing the activation distribution of subsequent tokens. Crucially, as these prefix tokens are independent of the user query, they do not convey any confidential information. As a result, their associated Key-Value states can be precomputed and deployed as a shared, static cache, minimizing runtime overhead.

LLMs exhibit heterogeneous dynamics across dimensions, leading to *dimension-wise outliers*: some coordinates are consistently more likely to be large. The rotation approach [AMC²⁴] leverages computational invariance to insert orthogonal transformations into the model without affecting its outputs. By multiplying hidden states and selected weight matrices by orthogonal rotations, large activation spikes are redistributed in smaller-magnitudes across all dimensions, mitigating heavy-tailed outlier dimension. Because the transformations are orthogonal, they can be algebraically fused into adjacent weight matrices, preserving the original computation graph and model outputs while reducing observed activation magnitudes.

Together, these techniques reduce the activation range relevant for non-linear tasks from approximately 2,400 down to 6 (see Table 1 and Table 2). From now on, we consistently apply these outlier mitigation techniques.

Table 2: Maximum linear layer output values with prefix and rotation optimizations.

Position	Baseline	+Prefix	+Rotation	+Prefix+Rotation
down-proj	310.56	12.14	14.86	1.92
o-proj	10.12	9.91	1.14	1.08
v-proj	5.89	5.88	4.60	4.74

Table 3: Perplexity of Llama models under different bit-precision settings.

Precision	Llama-2-7B	Llama-3-8B
2^{-9}	5.51	6.33
2^{-10}	5.49	6.15
2^{-11}	5.49	6.14
2^{-12}	5.49	6.13
Baseline (FP16)	5.49	6.13

3.2 Precision of computations

To establish the precision requirements for CKKS-based inference, we conducted simulated LLM inference in the clear. We developed a custom simulator by extending PyTorch’s fake quantization utility [PGM⁺19]. This simulator emulates encrypted execution by substituting floating-point operations with fixed-point arithmetic and injecting additive noise that characterizes CKKS-specific errors. This allows us to explore LLM accuracy under various noise budgets and identify the optimal CKKS precision configuration. Furthermore, the transformation embeds CKKS-specific primitives, such as bootstrapping and rotations, directly into the execution graph. By precisely mirroring the execution sequence and noise growth of actual CKKS ciphertexts, our analysis yields two critical design constraints: *precision* and *dynamic range*. Table 3 reports the simulation results used to identify a safe precision target. We observe that a 12-bit error budget exhibits no perplexity degradation compared to the FP16 baseline across both models. Based on this observation, we select 12-bit precision as our target setting for all subsequent experiments.

3.3 Impact on non-linear functions

The range statistics of the simulations provide that, for the input \mathbf{x} of step s of each layer L (e.g., SoftMax at 6-th layer), a coordinate-wise bound $\beta_{i;(s,L)} > 0$ on $|x_i|$, the i -th coordinate of \mathbf{x} .

A tight control on ranges can be put to two uses.

- In the case of steps based on polynomial approximation (RMSNorm, SiLU, Softmax), this allows us to decrease the degree d of the polynomial approximation, hence the multiplicative depth (equal to $\lceil \log(d+1) \rceil$) and the evaluation cost (dominated by $O(\sqrt{d})$ ciphertext-ciphertext multiplications using the Paterson-Stockmeyer algorithm). We use conservative bounds $\beta_{i;(s,L)}$, as an outlier would result in an even larger value after polynomial evaluation.
- When performing bootstrapping, a good control of the size of the slots of the input ciphertext is required to optimize the tradeoff between input size and precision. In that case, using raw bounds coming from the data collection stage is

sufficient, as an outlier will only result in limited precision loss.

In the case of Softmax, the statistics for input ranges allowed us to use an aggressively shallow design based on [CHK⁺24], yielding an 8-level strategy for the main computation, compared to 13 levels in [CHK⁺24]. In addition to bounds on the input ranges, we also use distributional information on the inputs to reduce the cost of the normalization steps. We discuss Softmax more precisely in Section 4.4.

3.4 Avoiding extended bootstrapping

CKKS bootstrapping assumes the real and imaginary part of its inputs to be in $[-1, 1]$; if this assumption is not fulfilled, the precision quickly degrades unless one resorts to high-precision bootstrapping approaches such as [BCC⁺22, CKSS25], with significant impact on the total evaluation cost.

Rather than resorting to such a strategy, we use a tradeoff between input magnitude and bootstrapping precision. Given a ciphertext $ct_{(s,L)}$ at the input of step s at layer L , the simulations described in Section 3.1 provide us with bounds $(\beta_{i;(s,L)})_{0 \leq i < N}$ for values in the different slots. We encode those values and their inverses as a plaintexts pt and pt^{-1} , respectively, and compute $pt \odot \text{bootstrap}_p(ct \odot pt^{-1})$, where bootstrap_p is a bootstrapping procedure with p bits of precision. This guarantees that the ciphertext being bootstrapped has all its slots in $[-1, 1]$; in compensation, the absolute precision of the resulting bootstrapping in slot i is reduced by $\log_2 \beta_{i;(s,L)}$ bits. We observe that this strategy makes sense only if the $\beta_{i;(s,L)}$ ’s are moderate, as else all precision would be lost: this is ensured by the outlier mitigations described in Section 3.1.

We note that if a slot value $(x_{(s,L)})_i$ in slot i happens to exceed the bound $\beta_{i;(s,L)}$, the total loss of precision is $\log_2(\beta_{i;(s,L)}) + 2 \log_2(x_{(s,L)} / \beta_{i;(s,L)})$,³ which usually remains acceptable if the bound is only mildly exceeded: the use of conservative bounds is not strictly required here.

4 Handling a Large Number of Input Tokens

The transformer block in LLM consists of two stages: prefill (a.k.a. summarization) stage and decode (a.k.a. generation) stage. The prefill stage is computationally more demanding, since it involves linear algebra operations in higher dimensions. Further, its cost grows with the input token length, making it difficult for FHE-based LLM to handle even moderately large input token length.

To handle this difficulty, we propose an heterogeneous chunked prefill framework. It consists of splitting the prefill stage into two components. The first one, which we call public prefill stage, uses a large input sequence and generates the KV caches. The second one, which we call private prefill stage, uses a smaller input sequence that updates the KV caches from the public prefill while generating the first token of LLM. With these two separate prefill stages, we first transact the public parts of the input in the clear and complete the summarization by transacting the private parts in encrypted state.

³The first summand is the same as just above; the second one comes from the fact values not in $[-1, 1]$ impact the sine function approximation quadratically in CKKS bootstrapping.

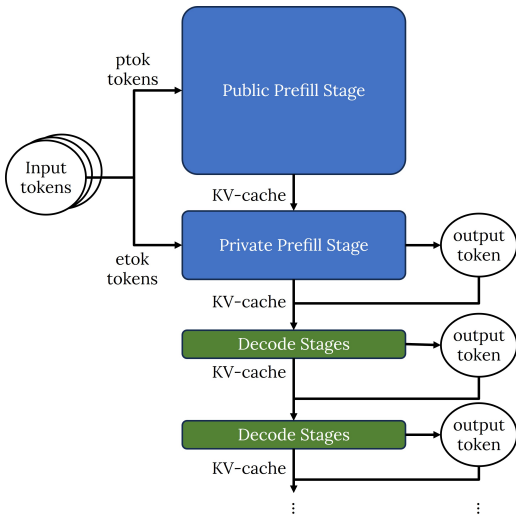


Figure 2: Visualization of the proposed plaintext algorithm with heterogeneous chunked prefill stages.

For the sake of efficiency of the FHE computations, we assume that the chunks are unbalanced. In particular, we consider the public prefill stage to be much larger than the private prefill stage. This is in contrast with most existing works on chunked prefills, which mainly focus on homogenous chunks [AKP⁺24].

In this section, we first describe our algorithm in clear in Section 4.1, and then explain how to homomorphically evaluate it in Section 4.2. Then, we focus on various components, which significantly improve the efficiency, in the rest of the section.

4.1 Plaintext algorithm

For the sake of simplicity, we first describe the algorithm without FHE. We first split the given input tokens of length $ntok$ into two components: a sequence of first $ptok$ input tokens and subsequent encrypted private $etok$ tokens. Then, our plaintext algorithm is as follows.

- **Public prefill stage:** it takes the first $ptok$ input tokens and generates the KV cache following the standard Llama prefill stage.
- **Private prefill stage:** it takes the subsequent $etok$ tokens and the KV cache from public prefill stage as inputs, and it updates the KV cache following the standard Llama prefill stage; it also outputs the first output token.
- **Decode stages:** they iteratively update the KV cache and generate tokens from the KV cache; they are exactly the same as the standard Llama decode stages.

Note that the public and private prefill stages are following the standard Llama prefill stages, but with different input lengths. The standard prefill algorithm uses $ntok$ tokens at once, and our chunked prefill stages use $ptok$ and $etok$ tokens, respectively. Figure 2 visualizes the proposed algorithm.

4.2 Encrypted computation overview

We now describe how to homomorphically evaluate the LLM inference as described in Section 4.1. The public prefill stage is performed in clear, and the decoding stage is analogous to the private prefill stage, with matrix-vector alternatives replacing matrix-matrix multiplications. We hence focus on the private prefill stage. It consists of four steps:

- (1) QKV-projection;
- (2) Attention Kernel;
- (3) O-projection;
- (4) FFN Kernel.

The first step, QKV-projection, is a composition of RMSNorm, PCMM and RoPE (RoPE is itself a plaintext-ciphertext multiplication, but fusing it with the PCMM would increase memory consumption). The third step, O-projection, also consists of PCMMs, along with an RMSNorm layer (Section 3). The last FFN step is a PCMM combined with SwiGLU (Section 3). For all PCMMs in those steps, we used algorithms from [BCH⁺24], which consume one level (see Section 2.1.4) and utilize fast BLAS libraries for improved efficiency.

Attention operation, the second step, requires more delicate algorithmic design. From the given encrypted QKV values and plain KV cache, the attention operation performs heavy matrix-matrix multiplications and Softmax's. There are two different types of processes involved. The first type is related to computations between the public KV cache and encrypted QKV values, and the second type is between the encrypted QKV values. We denote them as PC-attention and CC-attention, respectively.

The PC-attention utilizes plaintext-ciphertext operations, which are cheaper than ciphertext-ciphertext operations. Meanwhile, PC-attention takes as input a large plaintext KV cache (because it grows with $ptok$), and the overall circuit (including PCMM and Softmax) is wide. These two features imply that during PC-attention, (1) each (plaintext-ciphertext) operation is much cheaper than bootstrapping and (2) if we need bootstrapping, we may need many of them in parallel. Therefore, our rationale for the homomorphic computation of PC-attention is *to avoid bootstrapping as much as possible*.

⁴ To achieve a bootstrapping-thrifty PC-attention operation, we propose mostly-shallow homomorphic Softmax algorithm (Sections 4.4 and 4.5) and perform PCMM in slots to avoid the depth-consuming SlotToCoeff and CoeffToSlot operations. To evaluate PCMM in slots, we modify the algorithm from [JKLS18] and adapt it to consume less modulus and fewer key-switchings (Section 4.3).

The CC-attention consists of ciphertext-ciphertext operations and is relatively narrow. In CC-attention (like in QKV generation, O-projection, and FFN), we use bootstraps to handle the heaviest computations in the lowest moduli. In particular, we perform all heavy linear algebra in the lowest moduli possible with [JKLS18]: as these matrices have low dimensions, it seems preferable to use [JKLS18] rather than [Par25], while the other CCMM algorithm from [BCH⁺25] would require that one multiplicand is in

⁴In general, when homomorphically evaluating large circuits, bootstrapping can significantly reduce the cost. For example, it is often preferable to perform large matrix multiplication with the smallest FHE parameters possible and recover modulus afterwards using bootstrapping [BCH⁺24, Par25]. However, since PC-attention is wide, the cost of bootstrapping would be significant.

another encryption format. As the cost of linear algebra is comparable to that of bootstrapping, this strategy reduces the overall computational load.

Lastly, we homomorphically evaluate the decoding block stages analogously to the private prefill stage, but with matrix-vector operations instead of matrix-matrix operations. Specifically, we use the algorithms from [HYT⁺24] for PCMv in coefficients, and the algorithm from [HS14] for PCMv in slots.

Figure 3 summarizes the overall algorithm.

4.3 PCMM for PC-attention

Given our goal of achieving a bootstrapping-free PC-attention design, a first challenge lies in executing massive linear algebra operations without invoking bootstrapping. To this end, we propose a plaintext-ciphertext matrix multiplication variant of [JKLS18] that eliminates encoding state transitions and minimizes multiplicative depth.

Let A and B be matrices in $\mathbb{R}^{d \times d}$ and C be their product. The JKLS matrix multiplication algorithm relies on the following (plaintext) matrix equation:

$$C = \sum_{k=0}^{d-1} \text{Rot}_{\text{col}}^k(\sigma(A)) \odot \text{Rot}_{\text{row}}^k(\tau(B)) , \quad (2)$$

where \odot denotes the Hadamard (point-wise) multiplication between matrices stored as vectors by copying their rows one after another. Rot_{row} and Rot_{col} respectively represent rotation of row and column, and σ and τ represent relevant permutations. Specifically, we have, for all $0 \leq i, j < d$:

$$\begin{aligned} \left(\text{Rot}_{\text{col}}^k(A) \right)_{i,j} &= A_{i,j+k \bmod d} , \quad \left(\text{Rot}_{\text{row}}^k(A) \right)_{i,j} = A_{i+k \bmod d, j} , \\ (\sigma(A))_{i,j} &= A_{i,i+j \bmod d} , \quad (\tau(A))_{i,j} = A_{i+j \bmod d, j} . \end{aligned}$$

The original JKLS method homomorphically evaluates Equation (2) to obtain an encryption of C from encryptions of A and B . It consumes 3 multiplicative levels: one for σ and τ (performed in parallel), one for the column rotations (row rotations are implemented with a regular CKKS rotation and do not consume a level, if we write the matrix row after row in slots), and one for Hadamard multiplications.

Depth-optimized PCMM. Of course, PCMM can be viewed as a particular case of CCMM, and the corresponding *naive* JKLS algorithm for PCMM consumes three levels. By exploiting the fact that we focus specifically on PCMM, we reduce the multiplicative depth from 3 to 1. First, by setting A as the plaintext weight matrix and B as the ciphertext activation matrix, we remove one multiplicative level for the column rotations. Note that the plaintext column rotation is depth-free in terms of homomorphic computation.

Second, we adaptively update the packing structure of matrices to further reduce the multiplicative depth. Observe that the naive JKLS algorithm requires only one depth if the input matrix B is given as $\tau(\text{ct}_B)$ (instead of ct_B). From this observation, we modify the algorithm to take $\tau^{\ell+1}(\text{ct}_B)$ as an input and to output $\tau^\ell(\text{ct}_C)$, for an arbitrary integer ℓ .

LEMMA 4.1. *Let $M \in \mathbb{R}^{d \times d}$. For each integer k , we have:*

$$\tau \left(\text{Rot}_{\text{row}}^k(M) \right) = \text{Rot}_{\text{row}}^k(\tau(M)) ,$$

and

$$\tau \left(\text{Rot}_{\text{col}}^k(M) \right) = \text{Rot}_{\text{row}}^{-k} \circ \text{Rot}_{\text{col}}^k(\tau(M)) .$$

PROOF. Let $0 \leq i, j < d$. We have

$$\begin{aligned} \tau \left(\text{Rot}_{\text{row}}^k(M) \right)_{i,j} &= \left(\text{Rot}_{\text{row}}^k(M) \right)_{i+j,j} = M_{i+j+k,j} \\ &= (\tau(M))_{i+k,j} = \left(\text{Rot}_{\text{row}}^k(\tau(M)) \right)_{i,j} , \end{aligned}$$

and

$$\begin{aligned} \left(\tau \left(\text{Rot}_{\text{col}}^k(M) \right) \right)_{i,j} &= \left(\text{Rot}_{\text{col}}^k(M) \right)_{i+j,j} = M_{i+j,j+k} \\ &= (\tau(M))_{i-k,j+k} = \left(\text{Rot}_{\text{row}}^{-k} \circ \text{Rot}_{\text{col}}^k(\tau(M)) \right)_{i,j} , \end{aligned}$$

where all index operations are modulo d . \square

Using Lemma 4.1, we modify the original JKLS algorithm by applying τ^ℓ , to homomorphically compute $\tau^\ell(C)$ from $\tau^{\ell+1}(B)$.

THEOREM 4.2. *Let $A, B \in \mathbb{R}^{d \times d}$ and $C = A \cdot B$. For each integer ℓ , we have*

$$\tau^\ell(C) = \sum_{k=0}^{d-1} \left(\text{Rot}_{\text{row}}^{-\ell,k} \circ \text{Rot}_{\text{col}}^k(\tau^\ell \circ \sigma(A)) \right) \odot \left(\text{Rot}_{\text{row}}^k(\tau^{\ell+1}(B)) \right) .$$

PROOF. We apply τ^ℓ to both sides of Equation (2):

$$\begin{aligned} \tau^\ell(C) &= \tau^\ell \left(\sum_{k=0}^{d-1} \text{Rot}_{\text{col}}^k(\sigma(A)) \odot \text{Rot}_{\text{row}}^k(\tau(B)) \right) \\ &= \sum_{k=0}^{d-1} \tau^\ell \left(\text{Rot}_{\text{col}}^k(\sigma(A)) \right) \odot \tau^\ell \left(\text{Rot}_{\text{row}}^k(\tau(B)) \right) . \end{aligned}$$

Since the Rot_{row} and τ operators commute by Lemma 4.1, we have:

$$\tau^\ell \left(\text{Rot}_{\text{row}}^k(\tau(B)) \right) = \text{Rot}_{\text{row}}^k(\tau^{\ell+1}(B)) .$$

Moreover, Lemma 4.1 implies that

$$\begin{aligned} \tau^\ell \left(\text{Rot}_{\text{col}}^k(\sigma(A)) \right) &= \tau^{\ell-1} \left(\tau \left(\text{Rot}_{\text{col}}^k(\sigma(A)) \right) \right) \\ &= \tau^{\ell-1} \left(\text{Rot}_{\text{row}}^{-k} \circ \text{Rot}_{\text{col}}^k(\tau \circ \sigma(A)) \right) \\ &= \text{Rot}_{\text{row}}^{-k} \left(\tau^{\ell-1} \left(\text{Rot}_{\text{col}}^k(\tau \circ \sigma(A)) \right) \right) \\ &= \text{Rot}_{\text{row}}^{-2k} \left(\tau^{\ell-2} \left(\text{Rot}_{\text{col}}^k(\tau^2 \circ \sigma(A)) \right) \right) \\ &= \dots = \text{Rot}_{\text{row}}^{-\ell,k} \circ \text{Rot}_{\text{col}}^k(\tau^\ell \circ \sigma(A)) . \end{aligned}$$

This completes the proof. \square

Applying Theorem 4.2 to PCMM gives the following equation, corresponding to an algorithm that requires only one multiplicative level:

$$\tau^\ell(\text{ct}_C) = \sum_{k=0}^{d-1} \left(\text{Rot}_{\text{row}}^{-\ell,k} \circ \text{Rot}_{\text{col}}^k(\tau^\ell \circ \sigma(\text{pt}_A)) \right) \odot \left(\text{Rot}_{\text{row}}^k(\tau^{\ell+1}(\text{ct}_B)) \right) ,$$

where $\tau^\ell(\text{ct}_C)$ is the output ciphertext that decrypts to $\tau^\ell(C)$, and pt_A and $\tau^{\ell+1}(\text{ct}_B)$ are a plaintext and a ciphertext that respectively store input matrices A and $\tau^{\ell+1}(B)$.

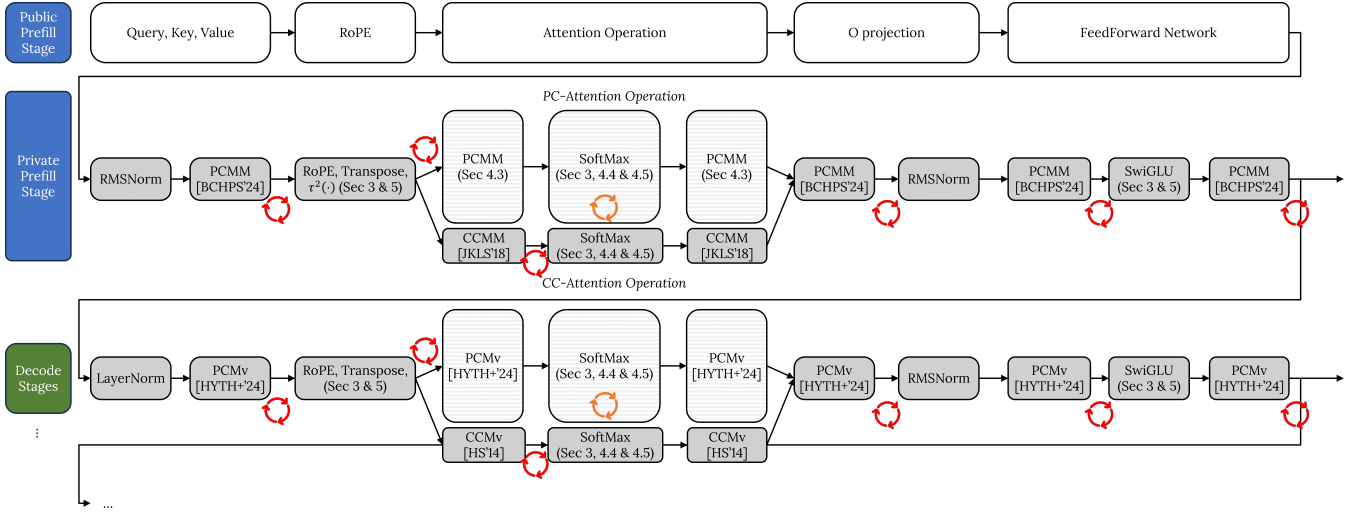


Figure 3: Overview of encrypted computation. The red and orange symbols indicate the bootstrap placements. The bootstrapping during Softmax evaluation (orange) is performed only in the narrow auxiliary track (see Section 4.4).

BSGS hoisting. We apply the Baby-Step Giant-Step (BSGS) technique to the rotations of ciphertext operand ct_B , reducing the number of ciphertext rotations from $O(d)$ to $O(\sqrt{d})$. Concretely, for arbitrary integers g, b with $g \cdot b = d$, we can compute $\tau^\ell(\text{ct}_C)$ as

$$\sum_{j=0}^{g-1} \text{Rot}_{\text{row}}^{j \cdot b} \left(\sum_{i=0}^{b-1} \text{pt}_{A,i,j,\ell} \odot \text{Rot}_{\text{row}}^i(\tau^{\ell+1}(\text{ct}_B)) \right), \quad (3)$$

where the plaintext matrix $\text{pt}_{A,i,j,\ell}$ is a rearranged version of pt_A defined as $\text{pt}_{A,i,j,\ell} = \text{Rot}_{\text{row}}^{-\ell \cdot (i+j \cdot b) - j \cdot b} \circ \text{Rot}_{\text{col}}^{i+j \cdot b}(\tau^\ell \circ \sigma(\text{pt}_A))$. The identity follows from the fact that the Rot_{row} and Rot_{col} operators commute.

The above equation gives an algorithm that computes $\tau^\ell(\text{ct}_C)$ from pt_A and $\tau^{\ell+1}(\text{ct}_B)$ using 1 multiplicative depth and $O(\sqrt{d})$ ciphertext rotations. We note that the plaintext operations on pt_A are depth-free.

On-the-fly PCMM. Equation (3) exploits a number of plaintext $\text{pt}_{A,i,j,\ell}$. However, since we are focusing on large models, the memory requirement for storing all the precomputed plaintexts is impractical. To tackle this issue, we store only $\tau^\ell \circ \sigma(\text{pt}_A)$ and compute $\text{pt}_{A,i,j,\ell}$ for each i, j and ℓ at runtime. This approach requires additional plaintext computations, but it significantly reduces the memory requirements. This is applicable to other PCMM (and PCMV) algorithms such as Powerperformer [PLL25] with a baby-step giant-step structure. However, our proposed PCMM algorithm requires fewer plaintext operations since each $\text{pt}_{A,i,j,\ell}$ can be obtained with only two plaintext rotations from $\tau^\ell \circ \sigma(\text{pt}_A)$.

Application to PC-attention. During PC-attention, we use the PCMM algorithm described above. In each step, a matrix M is encrypted as $\tau^\ell(M)$ for $\ell = 0, 1, 2$, stored row by row. More precisely, we apply $\tau^2(\cdot)$ during RoPE, and we store $\tau^2(M)$ after RoPE, $\tau^1(M)$ after the first PCMM in PC-attention, and $\tau^0(M)$ after the last PCMM in PC-attention for the relevant matrix M .

Note that we perform Softmax on $\tau(M)$:

$$(\text{Softmax}(\{(\tau(M))_{j,0}\}_j), \dots, \text{Softmax}(\{(\tau(M))_{j,d-1}\}_j)) .$$

Each vector $\{(\tau(M))_{j,i}\}_j$ is the i -th column of M rotated by i :

$$(M_{i,i}, \dots, M_{d-1,i}, M_{0,i}, \dots, M_{i-1,i}) ,$$

and the value $\text{Softmax}(\{(\tau(M))_{j,i}\}_j)$ is $\text{Softmax}(\{M_{j,i}\}_j)$ rotated by i . Therefore, as desired, the output is equivalent to

$$\tau(\text{Softmax}(\{M_{j,0}\}_j), \dots, \text{Softmax}(\{M_{j,d-1}\}_j)) ,$$

and one can continue with the subsequent PCMM.

4.4 A mostly-shallow Softmax

Our implementation of Softmax follows [CHK⁺24]. We briefly recall the main steps of this method. Let $(x_i)_{0 \leq i < d}$ be the input.

- Based on input range estimates, the input coordinates are translated to $[-M, 0]$ and scaled to $x'_i \in [-M/2^k, 0]$ for some real number M and integer k (for all $0 \leq i < d$); the identity $\text{Softmax}((x_i - a)_{0 \leq i < d}) = \text{Softmax}((x_i)_{0 \leq i < d})$ shows that translation has no impact on the result, whereas scaling is handled by the subsequent for loop;
- Using polynomial approximation over $[-M/2^k, 0]$, one computes $y_i^{(0)} = \exp(x'_i)$ for $0 \leq i < d$;
- For $1 \leq j \leq k$, one computes $y_i^{(j)} = (y_i^{(j-1)} / \|y_k^{(j-1)}\|_2)^2$; the inverse square root caused by the Euclidean norm in the denominator needs not be very accurate except at the last iteration (see [CHK⁺24]);
- One returns $(y_i^{(k)})_{0 \leq i < d}$.

The Softmax circuit is divided in two tracks: the main track includes all computations except for the normalization factors $1/\|y_k^{(j-1)}\|_2$, which are taken care of in an auxiliary track. The description above shows that the multiplicative depth of the main track is $2k$ and the depth consumption due to evaluating the exponential of the input values. Our mostly-shallow Softmax aims at avoiding bootstrapping

altogether in the main track, while allowing bootstraps only in the much more narrow auxiliary track.

The inverse square root computations of the third step can be performed either by polynomial approximation (as suggested in [CHK⁺24]), Newton’s method (as suggested in [MYJK²⁵]), or a combination of the two. Compared to the first, the second solution provides a deeper circuit, especially for a wide input interval; Newton’s method yields a cheaper computation than polynomial approximation, but its larger depth may require more bootstrappings when the input interval is wide.

In our present setting, we use the distributional data computed in Section 3.1 to obtain estimates on the range of the inverse square root computations that are sharper than the worst-case bounds used in [CHK⁺24]. These estimates allow us to restrict to $k = 2$ and degree-15 approximation for the exponential function; this yields a Softmax implementation using only 8 levels in its main track.

In order to minimize the number of bootstraps during the inverse square root computations, we use the polynomial approximation method from [CHK⁺24]. Given our aggressive choice of $k = 2$, we need to use degree-128 polynomials, which implies a high evaluation cost. As a single inverse square root computation is required per Softmax call, we notice following [CHK⁺24] that the slot usage is reduced by a factor ntok : the polynomial evaluation is performed on *slim ciphertexts*, namely ciphertexts which only use part of their slots.

4.5 Slim polynomial evaluation for Softmax

We introduce an algorithm that fully utilizes the SIMD property of CKKS to evaluate a polynomial of degree d on a ciphertext using only $\leq N/(2d)$ slots with $O(\log d)$ key-switching. An algorithm with the same goal was proposed in [OPP23]. It evaluates a polynomial by using the product decomposition $P(X) = p_d \prod_{0 \leq i < d} (X - \alpha_i)$, where the α_i ’s are the roots of the polynomial over an algebraic closure: to compute $P(x_0)$, start with $p_d^{1/d} (x_0 - \alpha_i)_{0 \leq i < d}$ in the slots, and rotate and multiply to accumulate the product. This algorithm was designed for exact homomorphic computations as supported by the BFV/BGV fully homomorphic encryption schemes [Bra12, FV12, BGV12]. Unfortunately, factoring the polynomial P as $P_1 \cdot P_2$ produces decompositions where both P_1 and P_2 take very large and very small values, leading to numerical instability and making this approach unsuitable for CKKS.

Polynomial decomposition. Our algorithm relies on the following lemma.

LEMMA 4.3. *Let $P \in \mathbb{R}[X]$ be a polynomial of even degree d with positive leading coefficient. There exist two polynomials U and V of degree $\leq d/2$ and a scalar m such that $P(x) = U(x)^2 + V(x)^2 - m$.*

PROOF. We set $m = \max_{x \in \mathbb{R}} (-P(x))$, which is finite under the assumption that P has a positive leading coefficient. Then $P + m$ is a polynomial taking only non-negative values. As a result, there exist two polynomials U and V such that $P + m = U^2 + V^2$ (see, e.g., [Ben17]). \square

Contrary to the factorization $P = P_1 \cdot P_2$, this decomposition guarantees that U and V cannot take very large values: for x in an interval \mathcal{I} , the values $|U(x)|$ and $|V(x)|$ are bounded from above by $\sqrt{\max_{x \in \mathcal{I}} |P(x)|} + m$.

We observe that two such polynomials can be computed from the roots of $P + m$ using an efficient algorithm described, e.g., in [Ben17]. Write $P + m = p_0 \prod_{i=0}^{d-1} (X - \alpha_i)$; as $P + m$ is a positive polynomial we can order the α_i ’s by pairs such that $\alpha_{2i} = \overline{\alpha_{2i+1}}$ (note that for our choice of m in the proof of Lemma 4.3, the root α_{2i} will be real for some i , but it then has even multiplicity). By using the identity

$$(X - \alpha_{2i})(X - \alpha_{2i+1}) = (X - \text{Re}(\alpha_{2i}))^2 + \text{Im}(\alpha_{2i})^2 ,$$

we obtain P as a product of sums of two squares. It then suffices to iteratively use the identity

$$\begin{aligned} (U_0^2 + V_0^2)(U_1^2 + V_1^2) &= \left(\frac{U_0 U_1 - V_0 V_1 + U_0 V_1 + U_1 V_0}{\sqrt{2}} \right)^2 + \\ &\quad \left(\frac{U_0 U_1 - V_0 V_1 - U_0 V_1 - U_1 V_0}{\sqrt{2}} \right)^2 \end{aligned} \quad (4)$$

to deduce the decomposition.

Note that Equation (4) is a variant of the decomposition $(U_0 U_1 - V_0 V_1)^2 + (U_0 V_1 + U_1 V_0)^2$ and that a variety of decompositions can be achieved by taking $\alpha^2 + \beta^2 = 1$ and writing

$$\begin{aligned} (U_0^2 + V_0^2)(U_1^2 + V_1^2) &= \\ &((V_1 U_0 + U_1 V_0) \alpha + (U_1 U_0 - V_1 V_0) \beta)^2 + \\ &((U_1 U_0 - V_1 V_0) \alpha + (V_1 U_0 + U_1 V_0) \beta)^2 . \end{aligned}$$

Polynomial evaluation. This gives the following encrypted algorithm for the evaluation of P : starting with a slim ciphertext ct encrypting $(m_i)_{0 \leq i < N/2}$ such that $m_{i+N/4} = m_i$, we evaluate U and V in parallel in slots of indices $0, \dots, N/4 - 1$ and $N/4, \dots, N/2 - 1$ to obtain ct' , and deduce the value of P by computing $\text{ct}' \odot \text{ct}' + \text{Rot}_{N/4}(\text{ct}' \odot \text{ct}')$. If the degrees of U and V are even, we can use the idea recursively: for a polynomial P of degree 2^k , we obtain a binary tree of polynomials. We define $U_0^{(0)}$ to be P . Let us fix a parameter j such that $0 \leq j < k$, and assume that we stop the recursion after j steps. For $0 \leq \ell \leq j$, the ℓ -th level of the binary tree contains polynomials $U_0^{(\ell)}, \dots, U_{2^{\ell-1}}^{(\ell)}$ of degree $2^{k-\ell}$ and constants $m_0^{(\ell-1)}, \dots, m_{2^{\ell-1}-1}^{(\ell-1)}$ such that

$$U_i^{(\ell)} + U_{i+2^{\ell-1}}^{(\ell)} = U_i^{(\ell-1)} + m_i^{(\ell-1)}, \quad 0 \leq i < 2^{\ell-1} . \quad (5)$$

For $0 \leq \delta \leq 2^{k-j}$, and given the number of slots 2^t of the target ciphertext such that $2^{t+j} \leq N$, we define the plaintext $v^{(\delta)}$ as containing in its slots $i2^t, \dots, (i+1)2^t - 1$ the degree- δ coefficient of the polynomial $U_{i \bmod 2^j}^{(j)}$. For $1 \leq \ell \leq j$, we define the plaintext $m^{(\ell-1)}$ as containing in its slots $i2^t, \dots, (i+1)2^t - 1$ the value $m_{i \bmod 2^{\ell-1}}^{(\ell-1)}$.

If we cut the tree at level j , we obtain Algorithm 1. This algorithm uses as a subroutine a function Evaluate which, on input a ciphertext ct encrypting $(m_i)_{0 \leq i < N}$ and plaintexts $v^{(0)}, \dots, v^{(2^j)}$ where $v^{(t)}$ encodes a vector $(v_i^{(t)})_{0 \leq i < N}$, returns ct' encrypting $\approx (\sum_{s=0}^{2^j} v_i^{(s)} m_i^s)_{0 \leq i < N}$. This function can be implemented using the Paterson-Stockmayer algorithm, using plaintext rather than scalars as polynomial coefficients.

THEOREM 4.4. *Algorithm 1 is correct. It uses $k+1$ multiplicative levels, and its cost is dominated by $O(2^{(k-j)/2}) + j$ ciphertext-ciphertext multiplications and j rotations.*

Algorithm 1 Slim polynomial evaluation algorithm for a polynomial of degree 2^k , with depth $j < k$ recursion, on input a slim ciphertext with 2^t slots with $2^{t+j} \leq N$.

Input: $\text{ct} = (a, b) \in \mathcal{R}_{Q_\ell}^2$
Input: Plaintexts $v^{(0)}, \dots, v^{(2^{k-j})}, m^{(0)}, \dots, m^{(j-1)}$
Input: Key-switching keys $\text{rlk}, (\text{rk}_{2^{t+i}})_{0 \leq i < j}$
Output: (a', b') .

- 1: $\text{ct} \leftarrow \text{Evaluate}(\text{ct}, v^{(0)}, \dots, v^{(2^{k-j})})$;
- 2: **for** ℓ from j down to 1 **do**
- 3: $\text{ct} \leftarrow \text{Mult}_{\text{rlk}}(\text{ct}, \text{ct})$
- 4: $\text{ct} \leftarrow \text{ct} + \text{Rot}_{\text{rk}_{2^{t+\ell-1}}}(\text{ct}, 2^{t+\ell-1}) - m^{(\ell-1)}$.
- 5: **end for**
- 6: **return** ct

By obtaining on input a ciphertext containing $\left(v_i^{(2^{k-j})}\right)^{2^{j-k}}$. ct_i by fusing a plaintext-ciphertext multiplication in a previous operation, Algorithm 1 can be made to use only k levels.

Numerical stability. As $|x^2 - y^2| \leq 2 \max(|x|, |y|) \cdot |x - y|$, every iteration of the main loop of Algorithm 1 introduces a numerical error of $\approx 1 + \log(|U_i^{(\ell)}(x)| + |U_{i+2^{\ell-1}}^{(\ell)}(x)|)$ bits in slot i .

As the proof of Lemma 4.3 shows that we can obtain different decompositions by changing the ordering of the roots of the polynomial P , it is thus preferable to search for a decomposition such that, at each level of the recursion, the polynomials U and V are small over the interval of approximation. In view of Equation (5), exploring the set of possible decompositions at step $\ell - 1$ in search of $U_i^{(\ell-1)}$ with a small associated $m_i^{(\ell-1)}$ is likely to yield polynomials $U_i^{(\ell)}$ and $U_{i+2^{\ell-1}}^{(\ell)}$ with smaller values at the next stage.

As a rule of thumb, our experiments suggest that Algorithm 1 loses 1 bit of precision per level; this can be accounted for by slightly increasing the scaling factor of the corresponding multiplicative levels.

5 Implementation

All experiments are conducted on a server equipped with eight NVIDIA RTX 4090 GPUs. The system uses an Intel Xeon Gold 6342 and 1TB of system memory, with all GPUs connected via PCIe Gen4. We developed our core system in C++ and CUDA, and auxiliary utilities in Python. The system interfaces with an FHE library for primitive operations and cryptographic setup. Throughout this paper, all experiments are conducted using the HEaaN2 library [Cry25]. For linear transformations, including PCMM, CCMM, PCMV, and CCMV, we implemented custom kernels within our system; these implementations are backend-agnostic and can be readily adapted to other FHE backends. For non-linear transformations, we either rely on Chebyshev polynomial evaluation or implement slim polynomial evaluation and Newton-type methods. For the LLM interface, we wrote a PyTorch C++-based extension.

5.1 Non-linear steps

We design polynomial approximations for SiLU and RMSNorm using standard Chebyshev approximation techniques. We set ranges and precision according to our plaintext experiments, adopting a

Table 4: Polynomial approximation strategies for non-linear functions.

Function	Polynomial Approx. Input Range	Polynomial Evaluation
SiLU	$[-16, 16], [-24, 24]$	Layer-wise + Dimension-wise
RMSNorm	$[1/\sqrt{30}, \sqrt{30}]$	Layer-wise

layer-wise approach for a sharper range control. In the case of SiLU, for optimal efficiency we adopt a dimension-wise approach, as some dimensions display outlier values, requiring a larger range than most.

Regarding Softmax, we refer the reader to Sections 4.4 and 4.5. Table 4 summarizes the ranges and approximation strategies tailored to other non-linear function; for RMSNorm, we display the global range after multiplication by a layerwise constant.

5.2 Linear algebra

Our algorithm involves various types of linear algebra operations (CCMM, PCMM, CCMV, PCMV, transpose) with various dimensions and batch sizes. As we describe in Figure 3, we carefully coordinate state-of-the-art algorithms [BCH²⁴, HYT²⁴, JKLS18] and devise a specific PCMM algorithms (Section 4.3) accordingly. For CCMV, we adopted algorithm from [HS14] with a diagonal packing. Transpose and $\tau^2(\cdot)$ are reduced to PCMV by seeing the relevant matrix as a vector and transposition and $\tau^2(\cdot)$ as linear maps operating on this vector.

Here are more details about the shape of linear algebra components. In the attention step, the hidden dimension of size 4096 is partitioned into 32 attention heads, each operating on an 128-dimensional subspace. We set the encrypted query size to 128 for computational efficiency, resulting in encrypted 128×128 matrices. Consequently, 32 independent matrix multiplications, corresponding to the number of attention heads, are executed concurrently, for both PCMM and CCMM. This computation pattern naturally maps to batched matrix multiplication, where multiple matrices are packed into a single ciphertext to fully utilize the available slots.

On the other hand, the linear algebra operations in the QKV/O-projection and FFN steps have limited parallelism (up to three concurrent matrices) but involve substantially larger dimensions (e.g., 4096, 11008 and 14336). This computation profile is better characterized as non-batched matrix multiplication over large dimensions, which necessitates a different algorithmic approach. To reduce computational complexity in these steps, we adopt coefficient-encoding-based algorithms [BCH²⁴, HYT²⁴] that allow computing heavy linear algebra with the smallest parameters possible.

For PCMM steps, we used Algorithm 2 from [BCH²⁴], which relies on MLWE ciphertext formats. Note that we use CKKS ring of degree 2^{16} while the dimensions of the PCMM tasks are $4096 \times 4096 \times 128$, $11008 \times 4096 \times 128$ and $4096 \times 11008 \times 128$ for Llama-2-7B ($14336 \times 4096 \times 128$, $4096 \times 14336 \times 128$ for Llama-3-8B). To do so, we use MLWE ciphertext formats of degree 256 and rank 256. We use real slots rather than complex slots, and the dimension of MLWE ciphertext format is doubled compared to [BCH²⁴].

For PCMv steps, we use the Rhombus MVM algorithm [HYT²⁴]. The target PCMv matrix dimensions are 4096×4096 , 11008×4096 , and 4096×11008 for Llama-2-7B (14336×4096 , 4096×14336 for Llama-3-8B). Similar to PCMM [BCH²⁴], we compute PCMv with the smallest parameters possible by performing it in the following steps:

- (1) Lower the total level to 4;
- (2) Perform SlotToCoeffs to level 1;
- (3) Decompose to RLWE degree 4096;
- (4) Perform Rhombus MVM;
- (5) Compose to RLWE degree 2^{16} ;
- (6) Half Bootstrap to the highest level.

Packing structure. Part of our linear operations are performed in slot-encoding, while other parts are performed in coefficient-encoding. The homomorphic conversion from one encoding to the other implies a bit-reversal permutation related to the Cooley-Tukey decomposition of the FFT. We explain how to handle this permutation in Appendix A.

Plaintext-plaintext operations. We implement the plaintext column rotation $\text{Rot}_{\text{col}}^i(\cdot)$ via a masked-rotation approach: $\text{Rot}_i(\cdot) \odot \mathbf{m}_i + \text{Rot}_{i-d}(\cdot) \odot \tilde{\mathbf{m}}_i$, where \mathbf{m}_i and $\tilde{\mathbf{m}}_i$ are plaintext column masks. Note that this is much faster⁵ than encoding $\text{Rot}_{\text{col}}(\cdot)$ each time.

We also introduce *square-root encoding strategy* for an efficient plaintext-plaintext multiplication. In part of our PCMM algorithm, we use plaintext-plaintext operations to generate relevant plaintexts with the same scale factor and modulus as the corresponding ciphertexts. By using *square-root encoding strategy*, we directly compute the output plaintexts without any rescale operation or NTT overhead.

Precisely, when we multiply two plaintexts, we encode the plaintext operands with a scale factor of $\sqrt{\Delta}$, where Δ is the ciphertext scale factor. Then, their product has a scale factor of Δ , and it does not require any rescaling. Note that this is possible since plaintexts do not contain encryption errors.

5.3 NCCL Parallelism

We used the NCCL library to parallelize the operations. In the summarization stage, the 16 matrices of dimensions 128×256 (for a total of 128×4096) are distributed equally across the GPUs. Except for RMSNorm and PCMM, each GPU computes each operation only for its assigned matrix. RMSNorm computes the sum of all the matrices before the InvSqrt step by NCCL reduction.

For MLWE PCMMs, all matrices affect the result and thus have to be broadcasted. We broadcast the total 128×4096 ciphertext matrix right before matrix multiplication. Each GPU then computes the matrix multiplication only for the assigned partial plaintext matrix. The partial plaintext matrix is assigned to the GPUs in a balanced manner.

In the generation stage, since the vector is small enough, we do not parallelize operations except matrix multiplications. For CCMv, the same method is used as for the MLWE PCMMs; we compute CCMv for the assigned partial ciphertext and aggregate to reconstruct the vector. For PCMv, we use Rhombus differently, depending on the dimensions. For plaintext matrices of dimensions

4096×4096 , 11008×4096 and 14336×4096 , the ciphertext is masked and each GPU is assigned $4096/8$ values as there are 8 GPUs. For all relevant number k of rows, we run Rhombus in dimensions $k \times (4096/8)$ and sum the results. For matrices of dimensions 4096×11008 or 4096×14336 , the ciphertext cannot be equally split, so we instead broadcast the ciphertext before Rhombus and split the plaintext matrix similarly to how we used parallelism for the MLWE PCMMs.

Table 5: Execution time breakdown of the second block in Llama-2-7B and Llama-3-8B on 8 RTX 4090 GPUs.

Phase	Llama-2-7B		Llama-3-8B	
	4 GPUs	8 GPUs	4 GPUs	8 GPUs
Summarization				
QKV-proj	0.461	0.371	0.429	0.352
Attention kernel	2.948	1.505	2.850	1.489
O-proj	0.254	0.226	0.260	0.170
FFN kernel	0.870	0.557	0.924	0.634
Total (s)	4.532	2.659	4.463	2.645
Generation				
QKV-proj	0.204	0.178	0.192	0.169
Attention kernel	0.725	0.629	0.722	0.628
O-proj	0.050	0.045	0.053	0.047
FFN kernel	0.203	0.173	0.243	0.215
Total (s)	1.182	1.025	1.210	1.059

5.4 Experimental results

Table 5 reports the execution time of individual layers in the Llama models; for an estimate of end-to-end computation time these figures should be multiplied by 32, giving 85s for summarization and 33s for generation. As described in Section 4.1, the QKV-projection stage consists of the sequence RMSNorm, QKV projection, bootstrapping, QK-RoPE, bootstrapping. The attention kernel then executes QK^{top} , SoftMax and SV .

6 Conclusion

To scale the input length, we considered user queries that have a privacy-sensitive component and a benign component, which translates into heterogeneous encrypted / cleartext input tokens. By developing specific algorithms for this setup and incorporating machine learning techniques to master the ranges and precision of intermediate variables, we were able to obtain Llama-2-7B and Llama-3-8B CKKS inference timings that outperform the state of the art while accepting much more input tokens.

We stress that our proof-of-concept implementation can still be improved by incorporating independent complementary techniques that have recently been proposed. For instance, we did not consider token sampling, for which solutions have been described in [RSS²⁵, LLK²⁵]. Also, CCMM operations consume a significant proportion of the overall time, and are typically batched: several of them are performed in parallel. New algorithms specifically developed for this task [GL25, CKL25] could be considered for accelerating this component of LLM inference.

⁵Each encoding requires number theoretic transform (NTT), which is costly.

Acknowledgments

This paper was edited for spelling and grammar using Grammarly and Overleaf’s AI Assist. We used ChatGPT for generating skeletons of tables in LaTeX.

References

[AKP⁺24] A. Agrawal, N. Kedia, A. Panwar, J. Mohan, N. Kwatrami, A. Tumanov, and R. Ramjee. Taming throughput-latency tradeoff in LLM inference with sarathi-serve. In *OSDI*, 2024.

[AMC⁺24] S. Ashkboos, A. Mohtashami, M. L. Croci, B. Li, P. Cameron, M. Jaggi, D. Al-istarth, T. Hoefler, and J. Hensman. QuaRot: Outlier-free 4-bit inference in rotated LLMs. In *NeurIPS*, 2024.

[APM⁺23] A. Agrawal, A. Panwar, J. Mohan, N. Kwatrami, B. S. Gulavani, and R. Ramjee. SARATHI: Efficient LLM inference by piggybacking decodes with chunked prefills. 2023. Available at <https://arxiv.org/abs/2308.16369>.

[BCC⁺22] Y. Bae, J. H. Cheon, W. Cho, J. Kim, and T. Kim. META-BTS: bootstrapping precision beyond the limit. In *CCS*, 2022.

[BCH⁺24] Y. Bae, J. H. Cheon, G. Hanrot, J. H. Park, and D. Stehlé. Plaintext-ciphertext matrix multiplication and FHE Bootstrapping: Fast and fused. In *CRYPTO*, 2024.

[BCH⁺25] Y. Bae, J. H. Cheon, G. Hanrot, J. H. Park, and D. Stehlé. Fast homomorphic linear algebra with BLAS. 2025. Available at <https://arxiv.org/abs/2307.09288>.

[Ben17] Y. Benoist. Writing positive polynomials as sums of (few) squares. *EMS Newsletter*, 2017.

[BGV12] Z. Brakerski, C. Gentry, and V. Vaikuntanathan. (leveled) fully homomorphic encryption without bootstrapping. In *ITCS*, 2012.

[BGV14] Z. Brakerski, C. Gentry, and V. Vaikuntanathan. (leveled) fully homomorphic encryption without bootstrapping. *ACM Trans. Comput. Theory*, 2014.

[Bra12] Z. Brakerski. Fully homomorphic encryption without modulus switching from classical GapSVP. In *CRYPTO*, 2012.

[CBH⁺22] T. Chen, H. Bao, S. Huang, L. Dong, B. Jiao, D. Jiang, H. Zhou, J. Li, and F. Wei. THE-X: Privacy-preserving transformer inference with homomorphic encryption. 2022. *ACL*.

[CCK⁺25] J. H. Cheon, H. Choe, M. Kang, J. Kim, S. Kim, J. Mono, and T. Noh. Grafting: Decoupled scale factors and modulus in RNS-CKKS. In *CCS*, 2025.

[CHK⁺18] J. H. Cheon, K. Han, A. Kim, M. Kim, and Y. Song. Bootstrapping for approximate homomorphic encryption. In *EUROCRYPT*, 2018.

[CHR⁺24] W. Cho, G. Hanrot, T. Kim, M. Park, and D. Stehlé. Fast and accurate homomorphic Softmax evaluation. In *CCS*, 2024.

[CKKS17] J. H. Cheon, A. Kim, M. Kim, and Y. Song. Homomorphic encryption for arithmetic of approximate numbers. In *ASIACRYPT*, 2017.

[CKL25] J. H. Cheon, M. Kang, and J. Lee. Fast batch matrix multiplication in ciphertexts. 2025. Available at <https://eprint.iacr.org/2025/1957>.

[CKP22] J. H. Cheon, W. Kim, and J. H. Park. Efficient homomorphic evaluation on large intervals. *IEEE Trans. Inf. Forensics Secur.*, 2022.

[CKSS25] H. Choe, J. Kim, D. Stehlé, and E. Suvanto. Leveraging discrete CKKS to bootstrap in high precision. In *CCS*, 2025.

[Cry25] CryptoLab. HEaaN2 library, 2025.

[CXS⁺25] K. Cheng, Y. Xia, A. Song, J. Fu, W. Qu, Y. Shen, and J. Zhang. Mosformer: Maliciously secure three-party inference framework for large transformers. In *CCS*, 2025.

[DjLZ⁺25] Y. Dong, W. j. Lu, Y. Zheng, H. Wu, D. Zhao, J. Tan, Z. Huang, C. Hong, T. Wei, W. Chen, and J. Zhou. PUMA: Secure inference of LLaMa-7B in five minutes. *Security and Safety*, 2025.

[FV12] J. Fan and F. Vercauteren. Somewhat practical fully homomorphic encryption. 2012. Available at <https://eprint.iacr.org/2012/144>.

[GJM⁺24] K. Gupta, N. Jawalkar, A. Mukherjee, N. Chandran, D. Gupta, A. Panwar, and R. Sharma. Sigma: Secure GPT inference with function secret sharing. *PETS*, 2024.

[GL25] C. Gentry and Y. Lee. Fully homomorphic encryption for matrix arithmetic. 2025. Available at <https://eprint.iacr.org/2025/1935>.

[HLL⁺23] X. Hou, J. Liu, J. Li, Y. Li, W.-j. Lu, C. Hong, and K. Ren. CipherGPT: Secure two-party GPT inference. 2023. Available at <https://eprint.iacr.org/2023/1147>.

[HS14] S. Halevi and V. Shoup. Algorithms in HElib. In *CRYPTO*, 2014.

[HYT⁺24] J. He, K. Yang, G. Tang, Z. Huang, L. Lin, C. Wei, Y. Yan, and W. Wang. Rhombus: Fast homomorphic matrix-vector multiplication for secure two-party inference. In *CCS*, 2024.

[JKLS18] X. Jiang, M. Kim, K. Lauter, and Y. Song. Secure outsourced matrix computation and application to neural networks. In *CCS*, 2018.

[JKS⁺25] S. Jayashankar, J. Kim, M. B. Sullivan, W. Zheng, and D. Skarlatos. A scalable multi-GPU framework for encrypted large-model inference. 2025. Available at <https://arxiv.org/abs/2512.11269>.

[KC25] A. Y. L. Kei and S. S. M. Chow. SHAFT: Secure, handy, accurate, and fast transformer inference. In *NDSS*, 2025.

[KS18] D. Kim and Y. Song. Approximate homomorphic encryption over the conjugate-invariant ring. In *ISISC*, 2018.

[LHG⁺25] W.-j. Lu, Z. Huang, Z. Gu, J. Li, J. Liu, C. Hong, K. Ren, T. Wei, and W. Chen. BumbleBee: Secure two-party inference framework for large transformers. In *NDSS*, 2025.

[LLK⁺25] L. Lim, J. Liu, V. Kalagi, A. El Abbadi, and D. Agrawal. Hyperion: Private token sampling with homomorphic encryption. 2025. Available at <https://eprint.iacr.org/2025/2318>.

[LPR10] V. Lyubashevsky, C. Peikert, and O. Regev. On ideal lattices and learning with errors over rings. In *EUROCRYPT*, 2010.

[LS15] A. Langlois and D. Stehlé. Worst-case to average-case reductions for module lattices. *Des. Codes Cryptogr.*, 75, 2015.

[MYJK25] J. Moon, D. Yoo, X. Jiang, and M. Kim. THOR: Secure transformer inference with homomorphic encryption. In *CCS*, 2025.

[OPP23] H. Okada, R. Player, and S. Pohmann. Homomorphic polynomial evaluation using galois structure and applications to BFV bootstrapping. In *ASIACRYPT*, 2023.

[Par25] J. H. Park. Ciphertext-ciphertext matrix multiplication: Fast for large matrices. In *EUROCRYPT*, 2025.

[PGM⁺19] A. Paszke, S. Gross, F. Massa, A. Lerer, J. Bradbury, G. Chanan, T. Killeen, Z. Lin, N. Gimelshein, L. Antiga, A. Desmaison, A. Kopf, E. Z. Yang, Z. DeVito, M. Raison, A. Tejani, S. Chilamkurthy, B. Steiner, L. Fang, J. Bai, and S. Chintala. PyTorch: An imperative style, high-performance deep learning library. In *NeurIPS*, 2019.

[PLL25] D. Park, E. Lee, and J. Lee. Powerformer: Efficient and high-accuracy privacy-preserving language model with homomorphic encryption. In *ACL*, 2025.

[RSS⁺25] D. Rho, S. Seo, H. Sung, C. Min, and E. K. Ryu. Traveling salesman-based token ordering improves stability in homomorphically encrypted language models. 2025. Available at <https://arxiv.org/abs/2510.12343>.

[SCKL24] M. Sun, X. Chen, J. Z. Kolter, and Z. Liu. Massive activations in large language models. In *COLM*, 2024.

[SSTX09] D. Stehlé, R. Steinfeld, K. Tanaka, and K. Xagawa. Efficient public key encryption based on ideal lattices. In *ASIACRYPT*, 2009.

[TLI⁺23] H. Touvron, T. Lavrill, G. Izard, X. Martinet, M.-A. Lachaux, T. Lacroix, B. Rozière, N. Goyal, E. Hambro, F. Azhar, A. Rodriguez, A. Joulin, E. Grave, and G. Lample. LLaMA: Open and efficient foundation language models, 2023. Available at <https://arxiv.org/abs/2302.13971>.

[TMS⁺23] H. Touvron, L. Martin, K. Stone, P. Albert, A. Almahairi, Y. Babaei, N. Bashlykov, S. Batra, P. Bhargava, S. Bhosale, D. Biket, L. Blecher, C. Canton-Ferrer, M. Chen, G. Cucurull, D. Esiobu, J. Fernandes, J. Fu, W. Fu, B. Fuller, C. Gao, V. Goswami, N. Goyal, A. Hartshorn, S. Hosseini, R. Hou, H. Inan, M. Kardas, V. Kerkez, M. Khabsa, I. Kloumann, A. Korenev, P. S. Koura, M.-A. Lachaux, T. Lavrill, J. Lee, D. Liskovich, Y. Lu, Y. Mao, X. Martinet, T. Mihaylov, P. Mishra, I. Molybog, Y. Nie, A. Poulton, J. Reizenstein, R. Rungta, K. Saladi, A. Schelten, R. Silva, E. M. Smith, R. Subramanian, X. E. Tan, B. Tang, R. Taylor, A. Williams, J. Xiang Kuan, P. Xu, Z. Yan, I. Zarov, Y. Zhang, A. Fan, M. Kambadur, S. Narang, A. Rodriguez, R. Stojnic, S. Edunov, and T. Scialom. Llama 2: Open foundation and fine-tuned chat models. 2023. Available at <https://arxiv.org/abs/2307.09288>.

[VSP⁺17] A. Vaswani, N. Shazeer, N. Parmar, J. Uszkoreit, L. Jones, A. N. Gomez, L. Kaiser, and I. Polosukhin. Attention is all you need. In *NeurIPS*, 2017.

[WFZ⁺] H. Wu, W. Fang, Y. Zheng, J. Ma, J. Tan, Y. Wang, and L. Wang. Ditto: Quantization-aware secure inference of transformers upon MPC. In *PLMR*.

[XLL⁺25] Y. Xue, L. Liu, Y. Luo, B. Sun, and S. Fu. PrivMLM: Efficient three-party multimodal large language model secure inference supported prompt privacy. In *ICNP*, 2025.

[XLS⁺23] G. Xiao, J. Lin, M. Seznec, H. Wu, J. Demouth, and S. Han. SmoothQuant: Accurate and efficient post-training quantization for large language models. In *ICML*, 2023.

[XTC⁺24] G. Xiao, Y. Tian, B. Chen, S. Han, and M. Lewis. Efficient streaming language models with attention sinks. In *ICLR*, 2024.

[YCD⁺25] L. Yang, J. Chen, W. Dai, S. Wang, W. Wu, and Y. Feng. ARION: Attention-optimized transformer inference on encrypted data. 2025. Available at <https://eprint.iacr.org/2025/2271>.

[YZL23] M. Yuan, L. Zhang, and X.-Y. Li. Secure transformer inference protocol. 2023. Available at <https://arxiv.org/abs/2312.00025>.

[ZWS⁺25] L. Zhang, X. Wang, J. J. Sim, Z. Huang, J. Zhong, H. Wang, P. Duan, and K. Y. Lam. MOAI: Module-optimizing architecture for non-interactive secure transformer inference, 2025. Available at <https://eprint.iacr.org/2025/991>.

[ZYH⁺25] J. Zhang, X. Yang, L. He, K. Chen, W.-j. Lu, Y. Wang, X. Hou, J. Liu, K. Ren, and X. Yang. Secure transformer inference made non-interactive. In *NDSS*, 2025.

A Handling Bit-Reverse

Our strategy for the attention phase requires performing some linear operations using slot-encoding, and some others using coefficient encoding. Moving from one to the other is accomplished via the SlotToCoeffs and CoeffToSlots steps, which amount to homomorphic DFT. For efficiency reasons, these steps are implemented using variants of the Cooley-Tukey decomposition, which implies bit-reverse on the coordinates of either the input or the output ciphertext.

In order to perform operations both on the slot-encoding and on the coefficient-encoding, we need to account for this permutation and properly shuffle the plaintext matrix to make it compatible. Let us denote the i -th number (slot or coefficient) of a ciphertext ct by $ct[i]$ and the bit reverse function with k bits by $\text{bitReverse}(x, k)$.

We describe the packing structure related to the implementation of the PCMM algorithm from [BCH⁺24]. Note that the encrypted matrices have a dimension of 128×4096 . First, split the matrix into $16 \times 128 \times 256$ matrices. Then, transpose each of the 128×128 square matrices and encode by reading each row of the 128×256 matrix in order. For convenience, we define the following function.

$$0 \leq x < 2^k, f(x, k) = \begin{cases} x/2 & \text{if } 2 \mid x \\ (x-1)/2 + 2^{k-1} & \text{if } 2 \nmid x \end{cases}$$

Since f sends the last bit of x to the highest bit, f is bijective. If we denote the 128×256 matrix as A and the encoded ciphertext as ct , we can write as follows.

$$ct[i + 128j] = A[i][f(j, 8)]$$

Denote the slot encoded ciphertext by ct_s , coefficient encoded ciphertext by ct_c (after Step 2), RLWE degree 4096 ciphertexts by ct_d (after Step 3), and the MLWE ciphertexts by ct_m (after Step 4). Then, the following is true.

$$\begin{aligned} ct_m[16i + j][k] &= ct_d[i][j + 16k] \\ &= ct_s[\text{bitReverse}(i + 16j + 256k, 15)] \\ &= ct_s[\text{bitReverse}(k, 7) + 128\text{bitReverse}(i + 16j, 7)] \\ &= A[\text{bitReverse}(k, 7)][f(\text{bitReverse}(i + 16j, 7), 8)] \end{aligned}$$

The matrix multiplication is along the second dimension of A . Therefore, we need to compute the permutation $g \in S_{256}$ given by

$$g(16i + j) = f(\text{bitReverse}(i + 16j, 7), 8)$$

After decomposing the integer into bits, we get the following representation of g .

$$g(\overline{a_7 a_6 a_5 a_4 a_3 a_2 a_1 a_0}_{(2)}) = \overline{a_3 a_4 a_5 a_6 a_7 a_0 a_1 a_2}_{(2)}$$

We observe that g is an involution since $g(g(x)) = x$. Thus, when we compute the ciphertext-plaintext matrix multiplication with ciphertext A and plaintext B , we first split the plaintext into 256×256 sized blocks $B_{k,l}$. Then, we shuffle the plaintext matrix into $B'_{k,l}[i][j] = B_{k,l}[g(i)][g(j)]$ and compute the total matrix multiplication by aggregating each PC-MM results of the blocks.

For the PCMV steps with [HYT⁺24], we also take the bit-reverse structure into account as follows. We shuffle the plaintext matrix by the permutation $h \in S_{4096}$ given by

$$h(x) = \begin{cases} \text{bitReverse}(x) & \text{if } x < 2048 \\ \text{bitReverse}(x - 2048) + 2048 & \text{if } x \geq 2048 \end{cases}$$

The function h fixes the highest bit and reverses all the other bits.